Domain wall fermions and applications

Pavlos M. Vranas * [a]

[a]Physics Dept., University of Illinois, Urbana IL 61801, USA

Domain wall fermions provide a complimentary alternative to traditional lattice fermion approaches. By introducing an extra dimension, the amount of chiral symmetry present in the lattice theory can be controlled in a linear way. This results in improved chiral properties as well as robust topological zero modes. A brief introduction on the subject and a discussion of chiral properties and applications, such as zero and finite temperature QCD, $\mathcal{N} = 1$ Super Yang-Mills, and four-fermion theories, is presented.

1. Introduction

When a continuum theory is regularized by the lattice the original number of fermion species is increased by 2^d, where d is the dimension of space-time, with a net chirality of zero. This is the well–known fermion doubling problem [1]. For vector theories like QCD, this problem has been traditionally treated at the expense of exact chiral symmetry by using Wilson [2] or Kogut-Susskind [3] fermions. Chiral symmetry is broken for any non-zero lattice spacing a, but is recovered together with Lorentz symmetry as $a \to 0$ resulting in the correct target theory in the continuum. However, since any numerical simulation is done at non-zero a, one must be able to simulate at small enough a so that the effect of the breaking does not obscure the underlying physics. The problem is that the computational cost of decreasing a is large. For example, in the full theory, decreasing a by a factor of 2 requires a factor of 2^{8-10} more computations.

In recent years an alternative lattice fermion method, domain wall fermions (DWF), has been developed and used in several applications. The method was introduced by D.B. Kaplan [4,6] and was further developed by Neuberger and Narayanan [5] and by Shamir and Furman [7,8]. Domain wall fermions are defined by extending space-time to five dimensions. A non–zero five dimensional mass m_0 is present. The size of the fifth dimension is L_s and free boundary conditions for the fermions are implemented. As a result the two chiral components of the Dirac fermion are separated with one chirality bound exponentially on one wall and the other on the opposite wall. For any lattice spacing the two chiralities mix only by an amount that decreases exponentially as $L_s \to \infty$. At $L_s = \infty$ chiral symmetry is exact even at non-zero a. In this way the continuum $a \to 0$ limit has been separated from the chiral $L_s \to \infty$ limit. Furthermore, the computing cost increases only linearly with L_s. Therefore, this method provides a new practical "knob" on the amount of chiral symmetry breaking due to the lattice discretization.

In order to have additional linear control over the "effective" fermion mass $m_{\rm eff}$, a four-dimensional mass m_f is introduced by explicitly mixing the plus chirality from one wall with the minus from the other. The parameters L_s, m_0 and m_f control the effective fermion mass $m_{\rm eff}$. In free one flavor theory one has [9]:

$$m_{\rm eff} = m_0(2 - m_0)[m_f + (1 - m_0)^{L_s}],\ 0\langle m_0\langle 2\,(1)$$

The $(1 - m_0)^{L_s}$ is a mass induced from the non zero overlap of the two chiral components. This residual mass becomes zero as $L_s \to \infty$. If $2 < m_0 < 4$ on has four flavors and if $4 < m_0 < 6$ six flavors. There is a symmetry around $m_0 = 5$. In the presence of increasing interactions these ranges get renormalized and shrink in size. Furthermore, the decay rate is not just the simple $-\ln(1 - m_0)$ of eq. 1 but also depends on the

*I would like to thank the Lattice 2000 organizers for their support and hospitality. Supported in part by NSF grant # NSF-PHY96-05199. Current address: IBM T.J. Watson Research Center, Route 134, Yorktown Heights, NY 10598, USA. vranasp@us.ibm.com.

gauge coupling in a complicated way.

The five dimensional theory contains L_s heavy species. For small L_s these would not affect the dynamics. However, as L_s is increased they may introduce bulk effects. These effects must be subtracted out by dividing the five-dimensional fermion determinant by the determinant of the same operator without domain walls, i.e. with anti-periodic boundary condition along the fifth direction [5]. This can be accomplished by introducing Pauli-Villars type fields as in [8] or with the modification [9]. Four-dimensional fermion fields $\overline{q}, q$ used in Green's functions are constructed from the $s = 0$ plus chirality and $s = L_s - 1$ minus chirality components of the five dimensional fields [8]. Gauge fields are introduced by treating the s direction as an internal flavor space [5,6]. They are only defined in four-dimensions, and they do not change along s. This construction is used by today's numerical simulations and is referred to as domain wall fermions.

Because the gauge fields are constant across the fifth direction s, the corresponding transfer matrix T is independent of s. Therefore, the product of the transfer matrices along s is simply T^{L_s}. For $L_s \to \infty$ this becomes a projection operator to the ground state defined by the corresponding four-dimensional Hamiltonian $\mathcal{H}$. It turns out that $\mathcal{H}$ is related to the hermitian Wilson Dirac operator $\gamma_5 D_W(m = -m_0)$ where D_W is the Wilson operator. Then the fermion determinant $\det D$ of the five dimensional theory contains a factor of the form $\langle b|0\rangle$. The boundary state $|b\rangle$ is independent of the gauge field and has fixed filling level while $|0\rangle$ is the ground state of $\mathcal{H}$ and its filling level depends on the gauge field. This construction is the overlap formalism [5] and has a powerful consequence. If the filling level of $|0\rangle$ is different from that of $|b\rangle$ their overlap is exactly zero. The fermion determinant $\det D$ can have exact and robust zero modes [5]! The corresponding index is simply the difference of the filling levels and is an integer. It turns out that:

$$\text{index} = (K_+ - K_-)/2 \tag{2}$$

where $K_\pm$ is the number of positive/negative eigenvalues of $\mathcal{H}$. For a finite lattice, $\mathcal{H}$ is a finite discrete matrix amenable to numerical analysis.

Even though on the lattice there is no topology in the strict sense it has been found that for smooth gauge field configurations the index theorem is obeyed exactly [5] and that for configurations generated by numerical simulations of a quantum theory the index theorem is obeyed in a statistical sense [10,11]. Also, it has been found that the zero mode properties are maintained to a good degree for relatively small L_s [12].

Unfortunately, the same property that makes DWF so attractive is also the reason for a weakness. When a configuration changes from one sector to another the number of negative eigenvalues of $\mathcal{H}$ changes and therefore an eigenvalue must cross zero. As a result T develops a unit eigenvalue. In that case there is no decay along s, the two walls do not decouple even as $L_s \to \infty$ and the chiral symmetry can not be restored. The set of configurations for which $\mathcal{H}$ has a zero eigenvalue is of measure zero and therefore this is not a problem [5,8]. However, configurations in their vicinity have very slow decoupling and as a result large values of L_s may be needed making the numerical simulations expensive. This is a problem for large lattice spacings (for $a^{-1} \approx 650$ MeV an $L_s \approx 100$ may be needed) but it diminishes rapidly as a becomes smaller (for $a^{-1} \approx 2$ GeV an $L_s \approx 20$ is adequate for most problems).

The subject of these proceedings is to report on work done during the past year relating to the chiral properties of DWF as well as to their applications in QCD and other vector-like theories; for reviews from previous years please see [13]

2. How many ways?

Before continuing it is important to put DWF into perspective. During the last few years a wealth of new lattice fermions with improved chiral properties have also been found. One could now wonder; How many different methods are there that solve the doubling problem for vector theories? Here is a list:

1) Wilson fermions, 1975 [2].
2) Kogut–Susskind fermions, 1975 [3].
3) Domain wall fermions, 1992-1994 [4–8].
4) Infinitely many fields, 1992, 1998 [14,15].
5) Overlap fermions, 1992-1994 [5]

6) Neuberger fermions, 1997 [16].
7) Perfect action fermions, 1997 [17].
8) Ginsparg-Wilson fermions, 1982, 1997 [18,19].
9) Molecule chains, 1999 [20].
10) Topological QFT in 5D, 2000 [21].

These methods are substantially different in appearance but they are of course related since they all describe the same continuum limit. Furthermore, even at finite lattice spacing many of these methods are intimately connected, some with exact analytical relations. Methods 3-10 share a common characteristic: in some limit of their parameters an "infinity" is present allowing exact chiral symmetry even at non-zero a.

One may think that such a proliferation of methods is unnecessary. However, further discoveries or improvements may come by exploiting these different ways of solving the same problem. The following is a quote from R. Feynman's "The Character of Physical Law" [22]: "Therefore psychologically we must keep all the theories in our heads, and every theoretical physicist who is any good knows six or seven different theoretical representations for exactly the same physics. He knows that they are all equivalent, and that nobody is ever going to be able to decide which one is right at that level, but he keeps them in his head, hoping that they will give him different ideas for guessing."

A list of references for works presented in this conference on new lattice fermions other than DWF is given in [35]-[54]. The reader should be aware that a large body of work on new lattice fermion methods is available.

3. Chiral properties

The chiral properties of DWF are determined by how well the chiral modes are localized on the walls. How fast the modes decay away from the wall is a dynamical property that depends on the other parameters of the theory such as couplings, masses, domain wall height, and volume, as well as the type of pure gauge action that is used. The broad properties of this dependence have been known for some time. However, work that was done during the past year has brought these properties into much sharper focus [55]-[73].

Before proceeding, it is interesting to see how the decay rate depends on the coupling constant, or equivalently the lattice spacing, in a simple case: the two flavor Schwinger model. In that model the chiral condensate $\langle\overline{q}q\rangle$ must be exactly zero if chiral symmetry is exact. A non zero value is a direct measure of breaking induced by the fermion regulator. In figure 1 $\langle\overline{q}q\rangle$ in units of the photon mass m_γ is plotted versus L_s. The data are from a dynamical numerical simulation [9]. From top to bottom they correspond to decreasing lattice spacings of $\sim 1/6$, $\sim 1/8$, $\sim 1/10$, and $\sim 1/12$. The physical volume is kept fixed. There are a few observations that can be made:

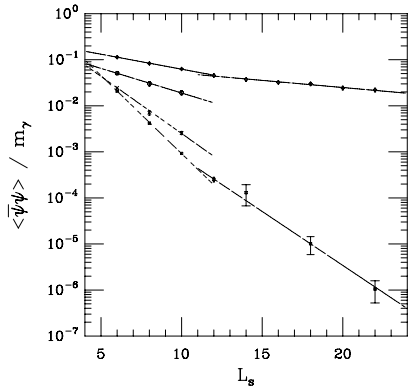

Figure 1. $\langle\overline{q}q\rangle$ in units of m_γ vs. L_s from a numerical simulation of the dynamical two flavor Schwinger model with $m_0 = 0.9$, $m_f = 0.0$ [9].

a) The data is consistent with exponential restoration of chiral symmetry.
b) There is a fast decay rate up-to $L_s \approx 10$, followed by a slower one for larger L_s. The analysis in [9] suggested that the fast decay rate is controlled by the fluctuations of the gauge field within a given topological sector, while the slower decay is associated with topology changing configurations. However, this also reflects the author's bias and does not exclude a variety of other possible decay functions.
c) Both decay rates become faster as the lattice spacing is decreased. This is important since otherwise numerical simulations with DWF would not be very attractive.

Probing the effects of finite L_s in QCD is much

more challenging because of spontaneous symmetry breaking. Much of the progress during the last year is due to inventive new probes that measure the residual mixing between the two walls. In a low energy effective Lagrangian sense one expects that this mixing will be reflected in the presence of an additive residual mass term $m_{\rm res}$ such that:

$$m_{\rm eff} = m_f + m_{\rm res}(S_G, \beta, L_s, m_0, m_f, V) \qquad (3)$$

where S_G is the form of the pure gauge action, $\beta = 6/g^2$ with g the coupling constant and V is the four-dimensional volume. The various approaches are:

i) From the pion mass:

$$m_\pi^2 \sim m_f + m_{\rm res}^\pi \Rightarrow m_\pi^2(m_f = -m_{\rm res}^\pi) = 0 \qquad (4)$$

ii) From PCAC [8] and fourth ref. in [13]

$$m_{\rm res}^R = \frac{\langle \sum_x J_{5q}^a(x, t \gg 1) J_{5q}^a(0,0)\rangle}{\langle \sum_x J_5^a(x, t \gg 1) J_5^a(0,0)\rangle} \qquad (5)$$

where J_5^a is the pseudo-scalar density, and J_{5q}^a is constructed from fields at $L_s/2$.

iii) Using the Gell-Mann-Oaks-Renner (GMOR) relation [8,62,67] one can fit $\langle \overline{q}q\rangle$ vs. m_f to the form:

$$(m_f + m_{\rm res}^G)\chi_\pi = \langle \overline{q}q\rangle - b_0 \qquad (6)$$

where χ_π is the pseudo-scalar susceptibility and b_0 is a constant.

iv) By fitting the eigenvalues Λ of the 5D hermitian DWF operator vs. m_f to the form:

$$\Lambda^2 = n^2[\lambda^2 + (m_f + \delta m)^2],\ \ m_{\rm res}^\Lambda = \langle \delta m\rangle \qquad (7)$$

where n, λ and δm are fit parameters [72].

v) By measuring the lowest eigenvalue $\lambda_{\rm min}$ of the 5D hermitian DWF operator only for configurations where the index is non-zero [60,64,58,57].

$$m_{\rm res}^\lambda = \langle \lambda_{\rm min}\rangle \qquad (8)$$

The index is measured using the overlap definition and the eigenvalue flow method [5]. For a non-zero index $\lambda_{\rm min}$ should be exactly zero in the $L_s \to \infty$ limit; for finite L_s the deviation from zero is a measure of chiral symmetry braking.

Using these probes the dependence of $m_{\rm res}$ on the parameters of the theory were studied in [55]-[73]. In the following, a collection of sample results from these references is presented. The figures are originals from the corresponding papers. When the symbols used in the figures are different from the ones in this article the correspondence will be noted in the figure caption.

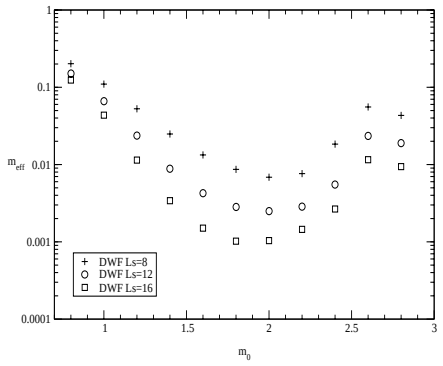

Figure 2. Quenched QCD; $m_{\rm res}^\lambda$ vs. m_0 from an 8^4, $\beta = 6.0$ configuration. From top to bottom $L_s = 8$, $L_s = 12$ and $L_s = 16$ [64].

The dependence of $m_{\rm res}$ on m_f is weak. For example, this can be clearly seen in [65]. The dependence on m_0 is shown, for example, in fig. 2 [64]. The value of m_0 is rather large except in a plateau region between 1.5 and 2.0. Also, in that region its value decreases faster with increasing L_s. The L_s dependence can be seen in fig. 3. The effect of chiral symmetry breaking decreases with increasing L_s. Also, an Iwasaki improved gauge action improves chiral symmetry substantially. The value of m_π at $L_s = 64$ with the standard plaquette action is reproduced with the Iwasaki action with L_s as small as 16. This will be further discussed in section 4.

Perhaps the most important issue about DWF has to do with the way the chiral limit is approached. The overlap guarantees that the chiral limit will be achieved as $L_s \to \infty$. However, it is possible that the allowed range of m_0 shrinks to zero size at strong coupling. In [63] a strong coupling calculation indicated that DWF lose their light state at very strong coupling. Also, in [71] it was found that in the large m_0 and strong coupling region DWF lose the light state. At weaker coupling the allowed range of m_0 is expected to be non-zero. But even then the precise way chiral symmetry is restored is not fully understood. Obviously this is very important because one would

like to be able to fit the data using the full functional form.

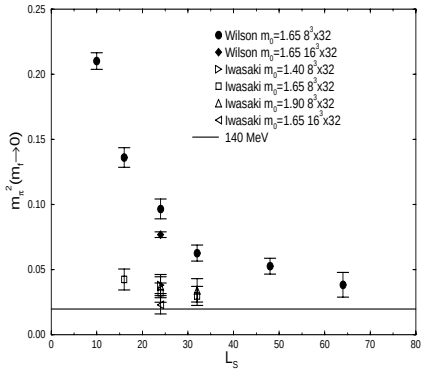

Figure 3. Quenched QCD; $m_\pi^2(m_f \to 0)$ vs. L_s with the plaquette action at $\beta = 5.7$ (filled) and the Iwasaki action (open) at $\beta = 2.2827$. [61,72].

The work of [11,23] indicates that the the spectrum of the 4-dimensional Hermitian Wilson operator has a non zero density around zero. Although that density decreases fast with decreasing lattice spacing it will induce some slow decay rates. This was also found in [70] where decay rates as small as 10^{-3} where observed. The work of [69,55] provides further insights: Results using the Wilson plaquette action for $a^{-1} \approx 1$ GeV and $a^{-1} \approx 2$ GeV are shown in fig. 4 while for the Iwasaki action and for the same lattice spacings in fig. 5. Also, data points from different volumes are shown indicating that the volume dependence is weak. Fits with exponential decay to zero were not good for $a^{-1} \approx 1$ GeV Wilson, $a^{-1} \approx 2$ GeV Wilson and $a^{-1} \approx 1$ GeV Iwasaki while fits with exponential decay to a constant were reasonable. For $a^{-1} \approx 2$ GeV Iwasaki an exponential fit to zero was reasonable.

More data points may be needed in order to precisely establish the form of chiral symmetry restoration as a function of L_s for different lattice spacings. It is possible that a more complicated function of L_s is required [9,76]. For example, in [72] several fitting functions were used including double exponentials.

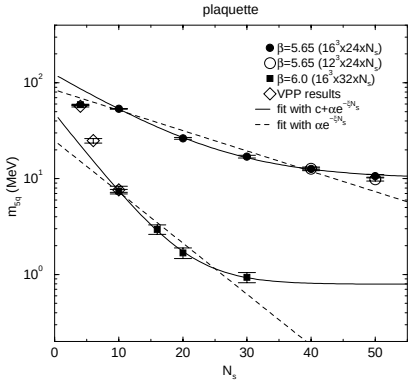

Figure 4. Quenched QCD; $m_{\rm res}^R$ vs. L_s with the plaquette action at $\beta = 5.65$ ($a^{-1} \approx 1$ GeV) and $\beta = 6.0$ ($a^{-1} \approx 2$ GeV) [69,55].

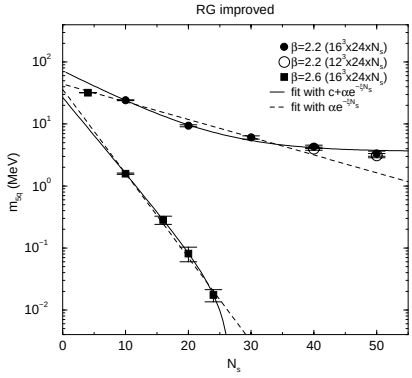

Figure 5. Quenched QCD; $m_{\rm res}^R$ vs. L_s with the Iwasaki action at $\beta = 2.2$ ($a^{-1} \approx 1$ GeV) and $\beta = 2.6$ ($a^{-1} \approx 2$ GeV) [69,55].

The above QCD results are for the quenched theory. The behavior of the dynamical theory has been studied in the context of thermodynamics. Similar results are evident there as can be seen from fig. 6.

The appeal of DWF is in the fact that any degree of chiral symmetry can be achieved even at finite lattice spacing (provided that the allowed m_0 region is not of zero size). However, in practice the required value of L_s may be large making the calculations difficult. An alternative approach was introduced in [72]. At finite L_s it is possible to approach the chiral limit by tuning m_f so that $m_f + m_{\rm res} = 0$. This approach is very similar to Wilson fermions. Even the Aoki phase is present for $m_f + m_{\rm res} < 0$ [73,24,65]. The same

chiral symmetry breaking terms are present but with much smaller coefficients.

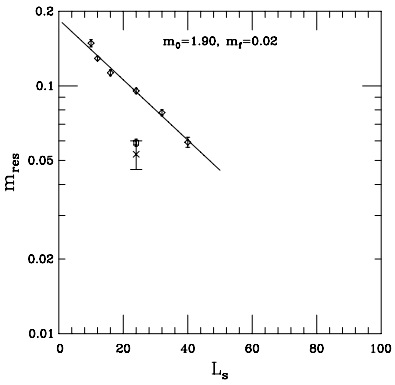

Figure 6. Dynamical QCD; $m^G_{\rm res}$ vs. L_s with the plaquette action on $8^3 \times 4$ lattices with $\beta = 5.2$, $m_f = 0.02$, and $m_0 = 1.9$ (diamonds). The cross/square are $m^G_{\rm res}/m^\pi_{\rm res}$ for $8^3 \times 32$, $\beta = 5.325$ ($N_t = 4$ crossover point) [62,67].

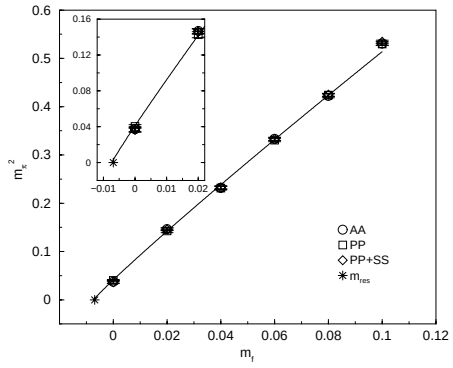

Figure 7. Quenched QCD; m^2_π vs. m_f with the plaquette action on $16^3 \times 32$ lattices with $\beta = 5.7$, $L_s = 48$, and $m_0 = 1.65$ [72,82]. The star indicates the $-m^R_{\rm res}$ point.

In fig. 7 [72,82] the approach of the pion mass to zero for quenched QCD is shown vs. m_f. This approach may be distorted by: order a^2 effects, finite L_s effects in the ultraviolet, topological near-zero modes (due to quenching), finite volume effects, and quenched chiral logs. In the quenched theory configurations with near zero modes are not suppressed by the fermion determinant. Because of the improved chiral properties of DWF the propagator has a near-pole as $m_f \to 0$ causing the pseudo-scalar pseudo-scalar (PP) correlator to diverge. This dramatic effect is shown in fig. 8 for $\langle \overline{q}q \rangle$ [72]. However, the coefficient of the divergent term is expected to vanish like $1/\sqrt{V}$ where V is the volume. This is evident in fig. 8 [72,86] (a similar divergence is present above the quenched deconfining transition but it does not disappear as V is increased [25]). Therefore, the pion mass extracted from the PP correlator for small volumes may be polluted. This can be alleviated by extracting the pion mass from the axial axial (AA) correlator instead [72].

Another pathology of quenching is the presence of quenched chiral logs. This can be accommodated by fitting to a function that contains a log as in fig. 7. This fit gives $m^\pi_{\rm res} = 0.0073(10)$ which is consistent with the value calculated using PCAC $m^R_{\rm res} = 0.0072(9)$ [72]. This provides a self-consistency check for the understanding of chiral symmetry breaking with DWF.

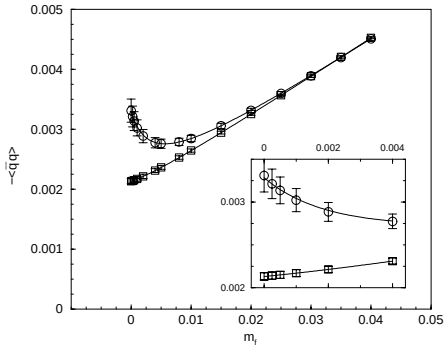

Figure 8. Quenched QCD; $-\langle \overline{q}q \rangle$ vs. m_f with the plaquette action on $8^3 \times 32$ (circles) and $16^3 \times 32$ (squares) lattices with $\beta = 5.7$, $L_s = 32$, and $m_0 = 1.65$ [72,86].

However, it must be stressed that $m_f + m_{\rm res} = 0$ does not eliminate all chiral symmetry breaking effects [86]. Power divergent operators introduce $O(m_{\rm res}/a^2)$ effects that must be subtracted out. These effects can be clearly seen in [86] where $f^2_\pi m^2_\pi / 48(mf + m_{\rm res})$ does not extrapolate to $\langle \overline{q}q \rangle (m_f + m_{\rm res} = 0)$.

4. Improvements

In this section improvements to DWF are discussed. The improved methods achieve the same

degree of chiral symmetry restoration but require less computing. Several methods have been developed during the last year [61,56,66,70], [74]-[77]. Also, work on locality properties during the past year can be found in [78]-[81].

As seen in section 3 the chiral properties of DWF are significantly better when an Iwasaki pure gauge action is used. This is remarkable; a change in the pure gauge action results in an improvement in the fermion sector. This is probably because the Iwasaki action "over-improves" and therefore reduces the frequency of index changes due to small instantons shrinking below the lattice spacing and disappearing. As mentioned in section 1, index changes result in slow decay rates. This is indicated by the work of [11] where it was found that index changes at values of m_0 where simulations are done are mainly due to small objects of size around the lattice spacing.

Using the Iwasaki action at $a^{-1} \approx 2$ GeV and $L_s = 20$ reduces $m_{\rm res}$ by a factor of 10 [69]. At $a^{-1} \approx 1$ GeV and $L_s = 20$ the improvement is not as dramatic, $m_{\rm res}$ is reduced by a factor of 2 [61,69]. At $a^{-1} \approx 650$ MeV, which is the lattice spacing around the $N_t = 4$ thermal transition, and $L_s = 24$, $m_{\rm res}$ reduces only by a factor of 1.2. Therefore, the Iwasaki action is effective at smaller a. QCD thermodynamics with $N_t = 4$ does not benefit much from it but at $N_t = 6$ ($a^{-1} \approx 1$ GeV) one would expect a factor of two improvement. Similar results have been obtained with other improved gauge actions [11,58].

If these interpretations are correct one would expect that actions used for "cooling" studies may be beneficial. For example, one could attempt to reduce index changes by "over-improving" the Iwasaki action even more. However, a study at $a^{-1} \approx 650$ MeV with an Iwasaki coefficient $c = -1$ instead of $c = -0.331$ did not show any significant further improvements [26]. Also, a study at $a^{-1} \approx 650$ MeV with an action that restricts the plaquette to $1 - {\rm Tr}[U_p]/3 < 0.8$ did not show significant further improvements either [27]. Nevertheless, these actions at smaller lattice spacings may produce better results.

Another set of improvements has to do directly with the fermion sector:
1) The projection method [66,77,70] consists of projecting out a few eigenvectors with the slowest decay rate. This method works remarkably well as can be seen from fig. 9.
2) An overlap inspired method introduces a different 5-dimensional operator [77]. Although the computational requirement is similar to DWF this method is better for analytical work.
3) A perturbation theory inspired method uses beyond nearest 4D neighbor action [76]. It has better decay rates at weaker couplings.
4) An algorithm that takes advantage of the absence of interactions along s uses multi-grid methods to speed-up computations [74].

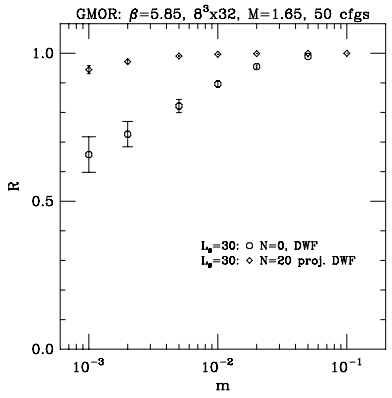

Figure 9. Quenched QCD; $R = m_f \chi_\pi / \langle \overline{q} q \rangle$ vs. m_f, where χ_π is the chiral susceptibility. R should be unity in the absence of chiral symmetry breaking. The bottom points are from unimproved DWF while the top are from improved DWF by projecting out the 20 slowest decaying eigenvectors [66,56].

5. Quenched QCD

Several applications of DWF to quenched QCD were done during the past year [82]-[95]. Most of them have been presented in the corresponding reviews but they are also mentioned here for completeness.

Calculations of $f_{\pi,K}$ have been made in [65,72] (see also the review [28]). For example, in [72] it was found that $f_{\pi,K}$ are close to the experimental values. Two different methods were used to calculate f_π; one used the PP correlator and the value of $m_{\rm res}^R$ while the other used the AA cor-

relator and did not require a value for $m_{\rm res}$. It was found that $(f_\pi)_{PP}/(f_\pi)_{AA} = 1.00(10)$. This provides a strong consistency check for the determination of $m_{\rm res}$.

A calculation of the nucleon to rho mass ratio [72] gave $m_N/m_\rho = 1.37(5)$ in the $a \to 0$ limit and for a box with size ≈ 1.6 fermi in each direction (the experimental value is 1.22). Also, the chiral condensate was measured to be $\langle\overline{q}q\rangle = (245(7)\ \text{MeV})^3$ at $L_s = 16$ and $\langle\overline{q}q\rangle = (256(8)\ \text{MeV})^3$ at $L_s = 24$ (the phenomenological estimate is $(229(9)\ \text{MeV})^3$).

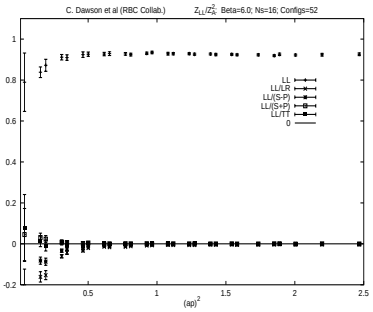

Figure 10. Quenched QCD; Non perturbative renormalization factors vs. $(ap)^2$ on a $16^3 \times 32$ lattice with $\beta = 6.0$, $L_s = 16$, $m_0 = 1.8$. The top points correspond to Z_{LL}/Z_A^2. The lower points correspond to factors that are zero when chiral symmetry is exact [91,89].

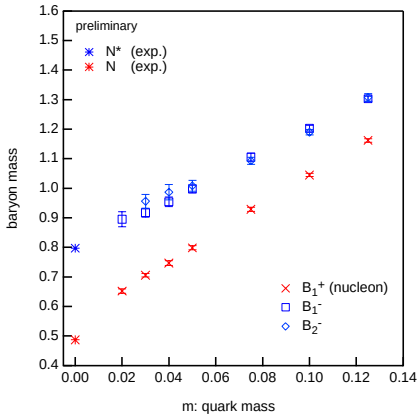

Figure 11. Quenched QCD; Baryon masses vs. m_f on a $16^3 \times 32$ lattice with $\beta = 6.0$, $L_s = 16$ and $m_0 = 1.8$ [93,87].

The renormalization factors relevant to weak matrix elements were calculated using non-perturbative methods in [91,89] (see also the review [29]). In fig. 10 one can see that the Z_{LL}/Z_A^2 factor is not zero as expected. The other factors in that figure are required to vanish if chiral symmetry was exact. Indeed, they are consistent with zero demonstrating the good chiral properties of DWF. Perturbative calculations of these factors were done in [34,65]. Also, a method that extends the range over which operators relevant to weak matrix elements are defined was developed in [88] (also see the review [29]).

The mass splitting between the nucleon $N(939)$ and its parity partner $N^*(1535)$ was calculated in [93,87] and is shown in fig. 11. The data are consistent with the experimental values.

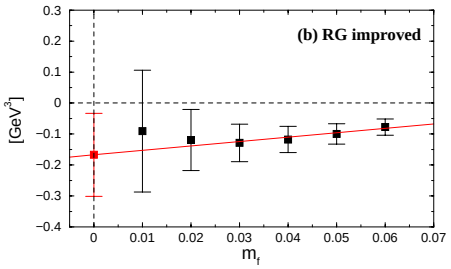

Figure 12. Quenched QCD; $Q_6^{(0)}$ vs. m_f with the Iwasaki action on $16^3 \times 24$ lattices with $\beta = 2.6$, $L_s = 16$, and $m_0 = 1.8$ [69,84].

The value of B_K was computed non-perturbatively in the RI scheme and matched to the $\overline{MS}$-NDR scheme in [85]. It was found to be $B_K(2\ \text{GeV}) = 0.538(8)$ on a $16^3 \times 32$ lattice with $L_s = 16$. This is lower than the value $B_K = 0.562(14)$ obtained by [83], probably because the non-perturbative renormalization constant of [85] is lower than the perturbative one used in [83] (see also the review [28]).

Operators relevant to $\epsilon\prime/\epsilon$ have also been calculated [84–86,89] (see also the review [28]). As an example the $Q_6^{(0)}$ operator is shown in fig. 12 [84]. The magnitude of this operator is small.

6. Dynamical QCD thermodynamics

The study of the QCD thermal transition can obviously benefit a great deal by using lattice fermions with better chiral properties. DWF are a natural candidate for such studies and have

been used over the past few years to study $N_t = 4$ thermodynamics. This effort crystallized during the past year [67,75], [96]-[102]. The main findings are:
1) A small but non-zero $U(1)_A$ symmetry breaking above and close to the transition is present. The good zero-mode properties of DWF lent validity to this result.
2) Two degenerate flavor simulations on $16^3 \times 4$ lattices with $L_s = 24$ gave a transition temperature of $T_c = 163(4)$ MeV and $m_\pi = 427(11)$ MeV, where the ρ mass was used to set the scale. Simulations with ordered and disordered starting configurations agreed after thermalization indicating the absence of a first order transition for this value of m_π.
3) Three degenerate flavor simulations on $16^3 \times 4$ lattices with $L_s = 24$ [30] gave a transition temperature of $T_c = 160(3)$ MeV and $m_\pi = 402(7)$ MeV. Again, simulations with ordered and disordered initial configurations indicated the absence of a first order transition for this value of m_π. The time history of these simulations at the crossover point is shown in fig. 13.

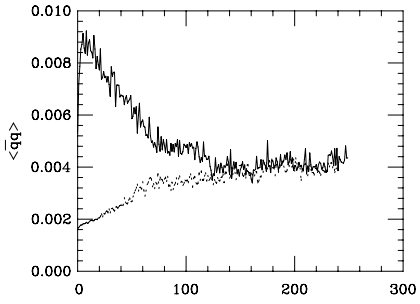

Figure 13. Dynamical QCD with 3 degenerate flavors; $\langle \overline{q}q \rangle$ vs. the trajectory number on a $16^3 \times 4$ lattice at the crossover point $\beta = 5.225$ with $L_s = 32$, $m_f = 0.02$ and $m_0 = 1.9$. The top data is from a disordered initial configuration while the bottom is from an ordered one [68].

Clearly, m_π is very large. From fig. 6 it was estimated that $L_s \approx 100$ may be needed to make $m_\pi \approx 200$ MeV. On the other hand, the transition with $N_t = 6$ will be at $a^{-1} \approx 1$ GeV. From quenched studies at $a^{-1} \approx 1$ GeV, see for example fig. 3, one would expect that the use of an Iwasaki action would be beneficial and that one could achieve $m_\pi \approx 200$ MeV with $L_s = 24$.

A study of the equation of state using DWF could be less demanding. One could integrate along the path proposed by G. Fleming [96]. Integrate from $\beta = 0$ to a β above the transition using the quenched theory which exactly corresponds to $m_f = 1$ because of the subtraction of the heavy fields. Keeping β fixed at that value one can then integrate along a line of decreasing m_f using the dynamical theory. Since this is done at realtively small a an $L_s \approx 24$ may be enough to make the calculation physically relevant.

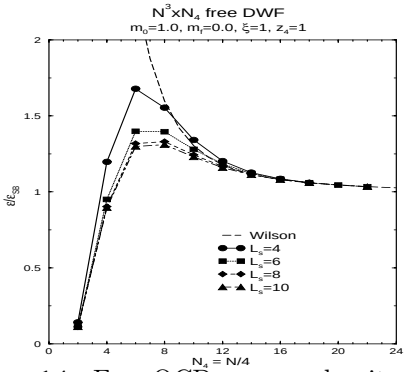

Figure 14. Free QCD; energy density ϵ on the lattice over the continuum Stefan-Boltzman energy density ϵ_{SB} vs. the number of sites along the time direction N_t. The spatial dimensions have $4N_t$ sites, $m_f = 0.0$, and $m_0 = 1.0$ [96].

In order to understand how good DWF are with $N_t = 4$ or even $N_t = 6$ the free fermion energy density is shown in fig. 14 [96]. Due to the subtraction of the heavy modes DWF perform better than Wilson fermions at small N_t.

7. Super Yang-Mills

The $\mathcal{N} = 1$ super-symmetric Yang-Mills (SYM) theory can be simulated on the lattice using traditional techniques, very much like in QCD. Simulations using Wilson fermions have already been performed, see for example [103]. However, these methods as in QCD, require fine tuning in order to recover the target theory in the continuum.

DWF offer an alternative [16,104] and [105]-[110]. At $m_f = 0$, $L_s \to \infty$ DWF forbid a

gluino mass term and because all other symmetry breaking operators are irrelevant SUSY is recovered in the continuum limit without fine-tuning. Furthermore, DWF for $m_f \geq 0$ have a Pfaffian (Pf) with definite sign for any gauge field configuration. This is important since in a numerical simulation the Pf is used as a Boltzmann weight which must be of definite sign. Wilson fermions at finite lattice spacing do not have a Pf of definite sign and numerical simulations are done with |Pf| instead. Since Pf in the $a \to 0$ limit has a definite sign one expects to recover the target theory but one may worry about non-analyticities resulting from taking the magnitude.

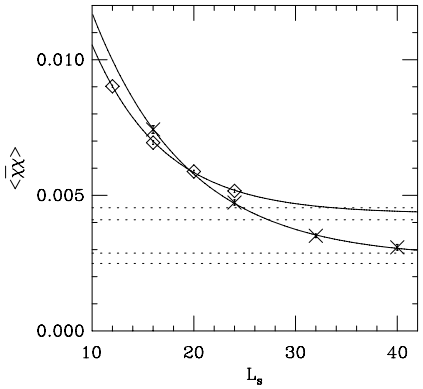

Figure 15. Dynamical $\mathcal{N} = 1$ $SU(2)$ super Yang-Mills; $\langle\overline{\chi}\chi\rangle$ vs. L_s with $m_f = 0$ and $m_0 = 1.9$. The diamonds are from an 8^4, $\beta = 2.3$ lattice while the crosses from 4^4, $\beta = 2.1$ [109,110].

For $\mathcal{N} = 1$ SYM the index is equal to $2\nu N_c$ where ν is the topological charge and N_c the number of colors. As a result, instantons break the $U(1)$ chiral symmetry down to Z_{2N_c} and an operator with $2N_c$ gluino fields acquires a vacuum expectation value. An interesting question is what happens to the remaining Z_{2N_c} symmetry. It is expected that Z_{2N_c} may break spontaneously to Z_2 [31]. However, on a torus there are constant field solutions with fractional topological charge $1/N_c$ [32]. Although for large volumes these solutions vanish, for small volumes they may play a role and induce a VEV even for zero mass. In particular, for $mV\langle\overline{\chi}\chi\rangle \ll 1$ the $\nu = \pm 1/N_c$ sectors exclusively contribute to $\langle\overline{\chi}\chi\rangle \neq 0$ [33].

Numerical simulations of $\mathcal{N} = 1$ SU(2) SYM were done in [109]. The results for $m_f = 0$ are shown in fig. 15. As can be seen, $\langle\overline{\chi}\chi\rangle(L_s \to \infty)$ has a non zero VEV which is maintained even for rather small volumes. The time histories of the 4^4 volume and $m_f = 0$ had "spikes" which are indicative of zero mode effects. These results seem to support a non-zero $\langle\overline{\chi}\chi\rangle$ due to configurations with fractional topological charge. Fractional topological charge configurations have already been found in the quenched theory [108].

8. Fermion–scalar interactions

All DWF fields across the extra direction interact the same way with the gauge field. The interaction of DWF with scalar fields was studied in [73] and was found to be different. That interaction takes place only along the link that connects the boundaries of the extra direction. This reveals a richness in the way different spin particles couple to DWF. Four-fermion models were studied using large N techniques and were supported by numerical simulations with N=2. It was found that the chiral properties of DWF in these models are good across a large range of couplings and that a phase with parity-flavor broken symmetry can develop for negative m_f if L_s is finite.

9. Conclusions

For the first time domain wall fermions separate the continuum ($a \to 0$) from the chiral ($L_s \to \infty$) limits. Since the computing requirement is only linear in L_s they provide practical control over chiral symmetry. Furthermore, they exhibit robust zero modes which become exact at the $L_s \to \infty$ limit.

DWF provide a complimentary alternative to traditional fermion methods and can shed light to different regions of the parameter space. DWF have found a large spectrum of applications such as: QCD thermodynamics, quenched QCD, Super Yang-Mills, four-fermion theories, and the Schwinger model. Also, there are proposals for improving DWF to achieve the same amount of chiral symmetry with less computations.

Finally, it should be noted that DWF are just one of the many new lattice fermion methods.

This wealth of approaches can only lead to further new discoveries.

REFERENCES

1. H.B Nielsen, M. Ninomiya, Nucl. Phys. **B185** (1981) 20.
2. K.G. Wilson, New Phenomena in Subnuclear Physics, ed. A Zichichi (Plenum Press, New York), Part A, (1975), 69.
3. J. Kogut, L. Susskind, Phys. Rev. **D11** (1975) 395.
4. D.B. Kaplan, Phys. Lett. **B288** (1992) 342.
5. R. Narayanan, H. Neuberger, Phys. Lett. **B302** (1993) 62; Phys. Rev. Lett. **71** (1993) 3251; Nucl. Phys. **B412** (1994) 574; Nucl. Phys. **B443** (1995) 305.
6. D.B. Kaplan, Nucl. Phys. **B30** (Proc. Suppl.) (1993) 597.
7. Y. Shamir, Nucl. Phys. B **406** (1993) 90.
8. V. Furman, Y. Shamir, Nucl. Phys. **B439** (1995) 54.
9. P.M. Vranas, Lattice 96, Nucl. Phys. **B53** (Proc. Suppl.) (1997) 278; Phys. Rev. **D57** (1998) 1415.
10. R. Narayanan and P. Vranas, Nucl. Phys. **B506** (1997) 373.
11. R. Edwards, U. Heller, R. Narayanan, Nucl. Phys. **B522** (1998) 285; Nucl. Phys. **B535** (1998) 403; Phys. Lett. **B438** (1998) 96.
12. P. Chen et. al., Phys. Rev. **D59** (1999) 054508.
13. R. Narayanan, Nucl. Phys. **B34** (Proc. Suppl.) (1994) 95; M. Creutz, Nucl. Phys. **B42** (Proc. Suppl.) (1995) 56; Y. Shamir, Nucl. Phys. **B47** (Proc. Suppl.) (1996) 212; T. Blum, Nucl. Phys. **B73** (Proc. Suppl.) (1999) 167. H. Neuberger, Nucl. Phys. **B83-84** (Proc. Suppl.) (2000) 67.
14. S.A Frolov, A.A Slavnov, Phys. Lett **309** (1993) 344.
15. A.A Slavnov, Nucl. Phys. **B544** (1999) 759, hep-lat/9807040.
16. H. Neuberger, Phys. Rev. **D57** (1998) 5417.
17. P. Hasenfratz, Nucl. Phys. **B63** (Proc. Suppl.) (1998) 53.
18. P.H. Ginsparg, K.G. Wilson, Phys. Rev bf D25 (1982) 2649.
19. M. Lüscher, Phys. Lett. **B428** (1998) 342.
20. M. Creutz, Phys. Rev. Lett. **83** (1999) 2636.
21. L.Baulieu, P.A.Grassi, D.Zwanziger, hep-th/0006036.
22. R. Feynman, "The character of Physical Law", MIT press 1985, p. 168.
23. R. Edwards, U. Heller, R. Narayanan, Phys. Rev. **D60** (1999) 034502.
24. T. Izubuchi, K. Nagai, Phys. Rev. **61** (2000) 094501.
25. Columbia collaboration, in preparation.
26. C. Christian, P. Vranas, in preparation.
27. G. Fleming, P. Vranas, in preparation.
28. L. Lellouch, these proceedings.
29. S. Sint, these proceedings.
30. Columbia collaboration, in preparation.
31. E. Witten Nucl. Phys. **B202** (1982) 253.
32. G. t'Hooft, Nucl. Phys. **B153** (1979) 141; Commun. Math. Phys. **81** (1981) 267.
33. H. Leutwyler, A. Smilga, Phys. Rev. **D46** (1992) 5607.
34. S. Aoki, T. Izubuchi, Y. Kuramashi, Phys. Rev **D59** (1999) 094505; Phys. Rev **D60** (1999) 114504;
35. U. Wenger, these proc., hep-lat/0011041.
36. P. Rüfenacht, these proc., hep-lat/0011041.
37. K. M. Holland, these proc., hep-lat/0010061.
38. Asit K. De, these proceedings.
39. S. Basak, these proc., hep-lat/0011018.
40. She-Sheng Xue, these proc., hep-lat/0010031.
41. G. Schierholz, these proceedings.
42. Keh-Fei Liu, these proceedings.
43. A. Slavnov, these proc., hep-lat/0010074.
44. S. Caracciolo, these proceedings.
45. L. Giusti, C. Hoelbling, C. Rebbi, these proc., hep-lat/0011014.
46. K. Holland, T. Joerg, these proc.,hep-lat/0010061.
47. Ting-Wai Chiu, these proc., hep-lat/0010070.
48. H. So, N. Ukita, these proc., hep-lat/0011050.
49. W. Bietenholz, these proc., hep-lat/0011012.
50. Christof Gattringer, hep-lat/0003005.
51. C. Gattringer, I. Hip, PL **B480** (2000) 112.
52. C. Alexandrou, E. Follana, H. Panagopoulos, E. Vicari, Nucl.Phys. B580 (2000) 394.
53. S.J. Dong, F.X. Lee, K.F. Liu, J.B. Zhang.
54. L.Giusti, C. Hoelbling, C.Rebbi, Nucl.Phys. **B83-84** (P.S.) (2000) 896.

55. K. Nagai, CP-PACS, these proc., hep-lat/0011032.
56. U. Heller, these proc., hep-lat/0010035.
57. C. Jung, these proc., hep-lat/0010094.
58. C. Jung, R. Edwards, X.Ji, V. Gadiyak, hep-lat/0007033.
59. L. Wu, RBC, these proc., hep-lat/0010098.
60. J.F. Lagae, D.K. Sinclair Nucl. Phys. **B83-84** (Proc.Suppl.) (2000) 405, hep-lat/9909097.
61. L. Wu, RBC, Nucl. Phys. B83-84 (Proc.Suppl.) (2000) 224, hep-lat/9909117.
62. G. Fleming, Columbia, Nucl. Phys. B83-84 (Proc.Suppl.) (2000) 363, hep-lat/9909140.
63. R. C. Brower, B. Svetitsky, Phys.Rev. D61 (2000) 114511, hep-lat/9912019.
64. V. Gadiyak, X. Ji, C. Jung, hep-lat/0002023.
65. S. Aoki, T. Izubuchi, Y. Kuramashi, hep-lat/0004003.
66. R. Edwards, U. Heller, hep-lat/0005002; private communication.
67. P. Chen et.al., Columbia collaboration, hep-lat/0006010.
68. Columbia collaboration, in preparation.
69. A. Ali Khan et. al., CP-PACS, hep-lat/0007014
70. P. Hernández, K. Jansen, M. Lüscher, hep-lat/0007015.
71. M. Golterman, Y. Shamir, hep-lat/0007021.
72. T. Blum et. al., RBC, hep-lat/0007038.
73. P. Vranas, I. Tziligakis, J. Kogut, hep-lat/9905018, Phys.Rev. D62 (2000) 054507.
74. A. Borici, hep-lat/9907003, Phys.Rev. D62 (2000) 017505.
75. P. Vranas, NATO workshop, Dubna, Russia, Oct. 1999, hep-lat/0001006.
76. Y. Shamir, hep-lat/0003024.
77. R. Narayanan, H. Neuberger, hep-lat/0005004.
78. P. Hernández, K. Jansen, M. Lüscher, hep-lat/9808010, Nucl.Phys. B552 (1999) 363.
79. Y. Kikukawa, T. Noguchi, hep-lat/9902022.
80. H. Neuberger, hep-lat/9911004, Phys.Rev. D61 (2000) 085015.
81. Y. Kikukawa, hep-lat/9912056.
82. M. Wingate, RBC, these proc., hep-lat/0009023.
83. Y. Taniguchi, CP-PACS, these proc., hep-lat/0010079.
84. J. Noaki, CP-PACS, these proc., hep-lat/0011007.
85. T. Blum, RBC, these proc., hep-lat/0011042.
86. R. Mawhinney, these proc., hep-lat/0010030.
87. S. Ohta, RBC, KEK, these proc., hep-lat/0011011.
88. Y. Zhestkov, these proc., hep-lat/0011002.
89. C. Dawson,RBC,these proc.,hep-lat/0011036.
90. T. Blum, A. Soni, M. Wingate, hep-lat/9902016, Phys.Rev. D60 (1999) 114507.
91. C. Dawson, RBC, hep-lat/9909107, Nucl.Phys.Proc.Suppl. 83-84 (2000) 854.
92. T. Blum, S. Sasaki, hep-lat/0002019.
93. S. Sasaki, RBC, KEK, hep-ph/0004252.
94. S. Aoki, Y. Kuramashi, hep-lat/0007024.
95. S. Ichinose, hep-th/9911079.
96. G. Fleming, these proceedings.
97. G. Fleming, Nucl. Phys. **A663** (2000) 979, hep-ph/9910453.
98. R. Mawhinney, Nucl. Phys. **B83** (Proc. Suppl.) (2000) 57, hep-lat/0001032.
99. P. Vranas, Columbia, Nucl. Phys. **B83** (Proc. Suppl) (2000) 414, hep-lat/9911002.
100. P. Vranas, DPF99, Los Angeles, hep-lat/9903024.
101. N. Christ et. al., ICHEP98, Vancouver Canada, July 98, hep-lat/9812011.
102. P. Vranas, Columbia, Nucl. Phys. **B73** (Proc. Suppl.) (1999) 456, hep-lat/9809159.
103. I. Montvay, Nucl. Phys. **B83-84** (Proc. Suppl) (2000) 188, and refs. within.
104. D.B. Kaplan, M. Schmaltz, hep-lat/0002030.
105. J. Nishimura, Phys.Lett. B406 (1997) 215, hep-lat/9701013.
106. S. Aoki, K. Nagai, S.V. Zenkin, Nucl.Phys. B508 (1997) 715, hep-lat/9705001.
107. T. Hotta, T. Izubuchi, J. Nishimura, Mod.Phys.Lett. A13 (1998) 1667, hep-lat/9712009.
108. R. Edwards, U. Heller, R. Narayanan, Phys.Lett. B438 (1998) 96, hep-lat/9806011.
109. G. Fleming, P. Vranas, J. Kogut, hep-lat/0008009.
110. G. Fleming, IVth Rencontres du Vietnam, July 19, 2000, Hanoi, Vietnam.